Developmental and Comparative Immunology 119 (2021) 104039

Contents lists available at ScienceDirect

Developmental and Comparative Immunology

journal homepage: www.elsevier.com/locate/devcompimm

Scavenger receptor B1 mediates phagocytosis and the antimicrobial peptide pathway in the endoparasitic wasp *Micropilits mediator*

Li-Zhen Zhou [a], Rui-Juan Wang [a], You-Ying Yan [a], Shuocheng Zeng [b], Zhen Zou [b], Zhiqiang Lu [a,c,*]

[a] Department of Entomology, College of Plant Protection, Northwest A&F University, Yangling, Shaanxi, China
[b] State Key Laboratory of Integrated Management of Pest Insects and Rodents, Institute of Zoology, Chinese Academy of Sciences, Beijing, China
[c] State Key Laboratory of Crop Stress Biology for Arid Areas, Northwest A&F University, Yangling, Shaanxi, China

ARTICLE INFO

Keywords:
Parasitic wasp
Scavenger receptor
Bacterial infection
Phagocytosis
Antimicrobial peptide

ABSTRACT

Scavenger receptors (SRs) are a family of pattern recognition receptors (PRRs) in the immune system. They are required for phagocytosis and act as co-receptors of Toll-like receptors to regulate immune signaling pathways in the fight against pathogens. Little is known about the function of SRs in insects. Here, we reported on a member of the SR family from the parasitic wasp *Micropilits mediator* (designated *Mm*SR-B1) that is responsive to bacterial infection. The recombinant extracellular CD36 domain of *Mm*SR-B1 produced in *Escherichia coli* cells is capable of binding to peptidoglycans and bacterial cells, causing agglutination of bacteria. Furthermore, we demonstrated that double-stranded RNA-mediated knockdown of *Mm*SR-B1 impedes hemocyte phagocytosis and down-regulates the expression of antimicrobial peptide (AMP) genes *defensins* and *hymenoptaecins*. Knockdown of *Mm*SR-B1 led to increased death of the wasps when challenged by bacteria. Our study suggests that *Mm*SR-B1 mediates phagocytosis and the production of AMPs in *M. mediator* wasps.

1. Introduction

Unlike vertebrates, insects lack adaptive immunity and rely on effective innate immunity to protect themselves from microbes, nematodes, and parasites. Once pathogens enter the insect hemocoel, circulating pattern recognition receptors (PRRs) specifically bind to pathogen-associated molecular patterns (PAMPs). Subsequently, humoral and cellular immunity modulate different signaling pathways (Buchon et al., 2014; Hillyer, 2016). In these processes, phagocytosis and antimicrobial peptides (AMPs) play key roles in the defense against invaders. Phagocytosis is a conserved cellular immune response that is mediated by hemocytes. This leads to the internalization of microbes by phagosomes, which are then fused with lysosomes to form phagolysosomes, in which pathogens are ultimately hydrolytically digested (Strand, 2008; Rosales, 2011; Hillyer and Strand, 2014). AMPs are effective humoral immune effector molecules produced in the fat body or epithelial cells in response to systemic infection. Activated Toll and immune deficiency pathways induce the transcription of AMPs, which are released into the circulatory system to destroy pathogens (Yi et al., 2014; Buchon et al., 2014; Hanson and Lemaitre, 2020).

PRRs are receptors that discriminate pathogens in the insect immune system, including gram-negative bacteria-binding proteins, peptidoglycan (PG) recognition proteins, thioester-containing proteins, lectins and scavenger receptors (SRs), and C-type lectins (Huang and Ren, 2020; Lu et al., 2020; Meng et al., 2019). Among them, the SR family has been extensively studied in vertebrates, but relatively few members have been reported in insects. SRs serve as transmembrane glycoproteins on the cell surface and were originally identified as low-density lipoprotein receptors on macrophages, owing to their uptake and chemical degradation of modified low-density lipoprotein through scavenger cell pathways (Gough and Gordon, 2000; Goldstein et al., 1979). The SR superfamily is divided into heterogeneous classes (A–I) according to their structural features. Class C members have been found only in invertebrates (Canton et al., 2013; Prabhudas et al., 2014). The domain architectures of different members determine the diverse functions of SRs. In addition to the clearance of modified lipoproteins, SRs participate in multiple physiological processes, such as signal transduction, phagocytosis, apoptotic cell elimination, cell adhesion, and antigen

* Corresponding author. Department of Entomology, College of Plant Protection, Northwest A&F University, Yangling, Shaanxi, China.
E-mail addresses: lizhenzhou@nwsuaf.edu.cn, lizhenZhou@nwsuaf.edu.cn (L.-Z. Zhou), wangruijuan1020@126.com (R.-J. Wang), 2019055087@nwafu.edu.cn (Y.-Y. Yan), zengshuocheng@ioz.ac.cn (S. Zeng), zouzhen@ioz.ac.cn (Z. Zou), zhiqiang.lu@nwsuaf.edu.cn (Z. Lu).

https://doi.org/10.1016/j.dci.2021.104039
Received 2 December 2020; Received in revised form 29 January 2021; Accepted 31 January 2021
Available online 4 February 2021

presentation (Canton et al., 2013).

SRs possess the ability to recognize conserved non-self PAMPs (Mukhopadhyay and Gordon, 2004; Peiser et al., 2004). In particular, Class B SRs (SR-Bs), which are comprised of SR-B1/SR-B2, CD36, and lysosomal integral membrane protein 2 from vertebrates, have been considered to mediate immune responses (Plüddemann et al., 2011; Silverstein and Febbraio, 2010; Prabhudas et al., 2014). SR-Bs are evolutionarily conserved glycoproteins that contain N- and C-terminal intracellular regions, two transmembrane domains, and an extracellular region with cysteine residues and N-linked glycosylation (Neculai et al., 2013; Prabhudas et al., 2014; Shen et al., 2014). SR-B1 possesses immunomodulatory properties to protect against sepsis, maintain lymphocyte homeostasis, and avoid autoimmune disorders (Zheng et al., 2014). In addition, SR-Bs act as co-receptors of Toll-like receptors (TLRs), playing a critical role in the initiation of the TLR-nuclear factor-κB signaling pathway to defend against invading microorganisms (Stewart et al., 2010; Wei et al., 2018). Similarly, the SR-B family has also been shown to promote bacterial clearance by AMP secretion and hemocyte phagocytosis in invertebrates (Bi et al., 2015; Tang et al., 2020). Studies in *Drosophila* have shown that SR-Bs are required for microbial binding and efficient bacterial clearance via phagocytosis (Kocks et al., 2005; Guillou et al., 2016).

Micropilits mediator, a species of endoparasitic wasp, is a natural enemy of many lepidopteran agricultural pests. In previous studies, we focused on the venom component and elucidated its function in parasitism (Lin et al., 2018, 2019). However, understanding the defense mechanism of parasitoids and preventing them from being threatened by microbial pathogens is conducive to maintaining their population. At present, physiological studies on parasitic wasps mainly focus on the interactions of parasitoids and their hosts; thus, the role of SRs in the immune systems of wasps remains largely unknown. In this study, we focused on an SR-B family member from *M. mediator*, denoted as *Mm*SR-B1. We investigated the expression profiles of *Mm*SR-B1 when the wasps were challenged by the gram-negative bacteria *Enterobacter cloacae* and gram-positive *Micrococcus luteus*. Recombinant *Mm*SR-B1 protein binds to bacterial cells and PGs from bacteria and curdlan, causing agglutination of bacterial cells. Knockdown of *Mm*SR-B1 resulted in decreased expression levels of AMPs, and hemocytes from *Mm*SR-B1-depleted wasps showed a reduced phagocytic response to bacteria. We analyzed the survival of *Mm*SR-B1-depleted wasps, and the results demonstrated that *Mm*SR-B1 is required for the wasps to survive bacterial infection. Collectively, our results revealed that *Mm*SR-B1 mediates immune signaling pathways and hemocyte phagocytosis in *M. mediator* wasps.

2. Materials and methods

2.1. Insect rearing

The endoparasitoid *M. mediator* population was originally obtained from the Institute of Zoology, Chinese Academy of Sciences (Beijing, China). Adult wasps were fed with 10% honey solution and maintained at 26 ± 1 °C, with 65 ± 5% relative humidity and a 14 h light/10 h dark cycle. The wasp host, armyworm *Mythimna separta*, was reared on fresh maize leaves (plant height of approximately 30 cm) under the same conditions. The second and third instar armyworm larvae were used as hosts for the wasps to maintain wasp generation in the laboratory.

2.2. Phylogenetic analysis

The amino acid sequences of SR-B homologs were compared using the Clustal X2.1 program and displayed with Bio-Edit software. Protein domains and signatures were predicted using InterPro (http://www.ebi.ac.uk/interpro/search/sequence). The transmembrane regions were predicted using TMHMM (http://www.cbs.dtu.dk/services/TMHMM). A phylogenetic tree was constructed using the unweighted pair-group method with arithmetic mean in the Geneious package with bootstrap resampling (1000 replicates).

2.3. Parasitoid infection by bacteria

Bacteria *Micrococcus luteus* (American Type Culture Collection 4698; Sigma-Aldrich, St. Louis, MO, USA) and *Enterobacter cloacae* (1.1016; China General Microbiological Culture Collection Center, Beijing, China) were cultured to an optical density ($OD_{600nm} \approx 0.8$) in Luria-Bertani medium at 37 °C with constant shaking at 250 rpm. Bacterial cells were collected by centrifugation at 5000×*g* for 5 min, washed 3 times with sterile phosphate-buffered saline (PBS), and then resuspended in sterilized PBS to 5×10^7 (*M. luteus*) and 5×10^4 (*E. cloacae*) colony-forming units (CFU)/mL. The second day adult wasps were anesthetized with CO_2 for 1 min and placed on ice. A capillary needle was dipped in the bacterial preparation for 2 s and immediately pricked into the abdomen of the wasps. The control group was treated with sterilized PBS (Wang et al., 2017).

2.4. Real-time quantitative polymerase chain reaction (RT-qPCR)

Total RNA was extracted from five wasps using Tripure reagent (Roche, Basel, Switzerland). RNA was reverse transcribed to complementary DNA (cDNA) using a Transcriptor First Strand cDNA Synthesis Kit (Roche) according to the manufacturer's instructions. RT-qPCR was performed using the KAPA SYBR® FAST qPCR Kit Master Mix (Kapa Biosystems, Wilmington, MA, USA) on a Rotor-Gene Q instrument (Qiagen, Hilden, Germany). The reaction conditions were as follows: 95 °C for 10 min, followed by 40 cycles of 95 °C for 10 s, 58 °C for 20 s, and 72 °C for 20 s. The *β-actin* gene was selected as the endogenous control (Wang et al., 2017). Data were obtained from four independent experiments and calculated using the $2^{-\Delta\Delta Ct}$ method (Schmittgen and Livak, 2008). The primers used in RT-qPCR were designed with Primer Premier 5.0 software and are listed in Table 1.

2.5. Prokaryotic expression and purification of MmSR-B1

The primers (r*Mm*SR-B1F and r*Mm*SR-B1R) used for amplification of the extracellular region of *Mm*SR-B1 were designed with Primer Premier 5.0 software. The amplification products were cloned into the pET-28a vector, which was digested by restriction endonucleases *Not*I and *Xho*I to develop the recombinant construct using the ClonExpress II One Step Cloning Kit (Vazyme, Nanjing, China). The recombinant plasmid pET-28a-*Mm*SR-B1 was transformed into *Escherichia coli* DH5α (Yeasen, Shanghai, China) and verified by sequencing. The verified plasmid pET-28a-*Mm*SR-B1 was transformed into *E. coli* BL21 (DE3; Yeasen) for recombinant protein expression. The positive single colony was cultured in Luria-Bertani medium containing kanamycin to the logarithmic phase ($OD_{600nm} \approx 0.6$) at 37 °C with shaking at 180 rpm. The *E. coli* cells were harvested after 4 h of induction with 0.5 isopropyl β-d-1-thiogalactopyranoside (IPTG). After brief sonication on ice, the inclusion bodies were obtained by centrifugation at 12,000×*g* for 10 min at 4 °C, re-suspended in PBS containing 8 M urea, and centrifuged again. The supernatant was loaded onto a Ni^{2+}-NTA column and eluted sequentially with imidazole buffer (10, 20, 50, 75, 100, 200, and 500 mM) containing 8 M urea. The eluted samples were examined by 10% sodium dodecyl sulfate polyacrylamide gel electrophoresis (SDS-PAGE) and stained with Coomassie Brilliant Blue R250 (Sigma-Aldrich). Purified *Mm*SR-B1 protein was collected and gradient dialyzed into urea buffer solution (PBS with 6, 4, 2, 1, and 0.5 M urea) to obtain renatured protein.

2.6. PAMP binding and bacteria agglutination assays

PGs from *Bacillus subtilis*, *Staphylococcus aureus*, and *E. coli K12* (InvivoGen, Toulouse, France) as well as curdlan from *Alcaligenes*

Table 1
Sequence of primers used in this study.

Primer names	Primer sequences (5'→3')
MmSR-B1	F: ACACAATAGCGCACCGAGAA
	R: CTGCTGAAGATGGCTGTCGA
Mmdefensin1	F: TCTCGTCGCCGGGATTTATG
	R: CCGGAGCTTCATAGTCGACC
Mmdefensin2	F: ACGTTCGTTTACCTCGAGCT
	R: GACCCCTTTTTCGCACCAAC
Mmlysozyme1	F: ACCGTTTCGCTCAGGATTGT
	R: GCAGGTTCTGTAGGCGTTCT
Mmlysozyme2	F: ATGCGAAGATTTTGCCGACG
	R: ATCCACTGACGTTGGGAAGC
Mmhymenoptaecin1	F: ATTAGTCGCATTAGTTTGTG
	R: CAGGATTGAATGGTGGTAT
Mmhymenoptaecin2	F: TTTCGTCCACAGATTTCA
	R: ATCCGGCCAGTGGGTAAT
Mmβ-actin	F: GGCCCCATCAACCATCAAGA
	R: GGACCGGATTCGTCGTACTC
ds*SR-B1*	F: TAATACGACTCACTATAGGGGTGTTCAATGCTTTTCCCGT
	R: TAATACGACTCACTATAGGGCAATGTTGTGGCGAATTTTG
ds*GFP*	F: TAATACGACTCACTATAGGGGTGTTCAATGCTTTTCCCGTTATCC
	R: TAATACGACTCACTATAGGGAGGTAATGGTTGTCTGGTAAAAGGA
rMmSR-B1	F: CGACAAGCTTGCGGCCGCATCATGGAAATATTGATAAATCG
	R: GTGGTGGTGGTGCTCGAGTCATGCTATCGGAGGCACTTCGACAGCC

The T7 promoter sequence is shown by underlines. F: Forward; R: Reverse; ds: double-strand; r: recombinant.

faecalis (Sigma-Aldrich) were used for the binding assay. In addition to these PAMPs, bacterial *M. luteus* and *Pseudomonas aeruginosa* (PAO1) cells were used for the binding assay. Twenty microliters of PAMPs (1 mg/mL) or bacterial cells (2×10^7 cells/mL) in PBS were incubated with 40 μL renatured *Mm*SR-B1 protein (150 μg/mL) and placed on a three-dimensional rotator for 2 h at room temperature. After centrifugation at 10,000×*g* for 10 min at 4 °C, the supernatant was used as an unbound sample, and the bound sample (PAMPs or bacterial cells) was collected and resuspended in PBS after washing with PBS containing 50, 150, or 500 mM NaCl (Chen et al., 2016). These samples were mixed with SDS loading buffer, prepared at 100 °C for 5 min, and then separated by 10% SDS-PAGE. The proteins on the gel were transferred to a polyvinylidene fluoride membrane and incubated with anti-His-tag monoclonal antibody (1:5000 dilution; Cwbio, Beijing, China) and goat anti-mouse IgG antibody (1:10,000 dilution; Cwbio). The bands were visualized using a chemiluminescence imaging system (Clinx, Shanghai, China).

For the bacterial agglutination assay, green fluorescent protein (GFP)-expressing *P. aeruginosa* (PAO1) and *E. coli* (DH5α) cells were used to detect whether *Mm*SR-B1 protein could induce agglutination of bacteria. The assay was performed as previously described (Chen et al., 2016) with some modifications. The tested bacteria were cultured in LB medium to the logarithmic phase ($OD_{600nm} \approx 0.8$) and washed three times with PBS. The bacterial samples (2×10^7 cells/mL in PBS) and renatured *Mm*SR-B1 protein (150 μg/mL) were mixed in a 96-well plate at a ratio of 1:2. In the control group, bovine serum albumin (BSA; 150 μg/mL) was used. After 2 h of incubation at room temperature, images were captured using a Nikon DS-Ri2 inverted fluorescence microscope (Nikon, Tokyo, Japan).

2.7. Double-stranded RNA (dsRNA) synthesis and RNA interference (RNAi)

Specific primers with the T7 promoter sequence (http://www.flyrnai.org/cgi-bin/RNAi_find_primers.pl) were used for PCR amplification (Table 1). The PCR products were purified with a Gel Extraction kit (Omega Bio-tek, Norcross, GA, USA) and used as templates for dsRNA synthesis. DsRNA was synthesized using the T7 RiboMAX Express RNAi System (Promega, Madison, WI, USA). The amplification product of GFP was cloned from the pGLO vector and used for the synthesis of dsGFP, which was used to control RNAi.

The second day adult wasps were injected with dsRNA (0.2; 8 μg/μL) in the abdomen using a Nanoject III micro-injector (Drummond Scientific, Broomall, PA, USA). Wasps injected with dsGFP served as the control group. After injection, the wasps were placed in clean containers and kept at 16 °C. The RNAi efficiency of *Mm*SR-B1 was examined using RT-qPCR.

2.8. Antibacterial peptide gene expression analysis

The second day adult wasps were anesthetized and infected as described above. The control group was treated with sterilized PBS. At 12 h post-infection, 5 wasps in each group were collected and stored at −80 °C. Antibacterial peptide genes (*defensin 1*, *defensin 2*, *lysozyme 1*, *lysozyme 2*, *hymenoptaecin 1*, and *hymenoptaecin 2*) were identified from the transcriptome data of *M. mediator* (unpublished). RT-qPCR was performed to determine the expression levels of these antibacterial peptide genes. Four biological replicates were used. To determine whether *Mm*SR-B1 had an impact on the expression levels of antibacterial peptide genes, wasps were infected at 3 days post-RNAi, and samples were collected at 12 h post-infection. The mRNA expression levels of the antibacterial peptide genes were determined by RT-qPCR. Three biological replicates were used.

2.9. Phagocytosis assay

For the *in vitro* phagocytosis assay, Alexa 594-labeled *E. coli* (K-12 strain) and *S. aureus* (Wood strain without protein A) BioParticles® conjugates (Invitrogen, Carlsbad, CA, USA) were prepared as suspensions of 1 mg/mL. At 4 days post-RNAi, the hemolymph was collected from the abdomen of each wasp using a capillary needle. Hemolymph samples from 15 to 20 wasps were added to a drop of Grace's medium (Invitrogen) containing 1 μL of 1% 1-phenyl-2-thiourea (Sigma-Aldrich). The prepared hemolymph samples were added to tissue culture-treated coverslips and placed in a 48-well cell culture plate (Invitrogen). The samples were left at room temperature for 3 h to allow the cells to adhere to coverslips, and then the medium was gently aspirated. Grace's medium was mixed with 1 μL of fluorescent-labeled bacterial suspension and added to the coverslips. The cell culture plate was kept in the dark for 1 h at room temperature, gently washed 2 times with Grace's medium, fixed with 4% paraformaldehyde for 10 min, and washed 3 times with PBS. To facilitate subsequent staining of the cytoskeleton, hemocytes were permeabilized with 0.5% Triton X-100 for 10 min and

washed again. SF488 phalloidin (Solarbio, Beijing, China) was used to stain F-actin in hemocytes for 1 h at room temperature. After washing with PBS 3 times, the cell nuclei were stained with Hoechst 33342 (Solarbio) for 10 min. The washed coverslips were turned over and placed on slides with Antifade Mounting Medium (Solarbio) (Ma et al., 2020). The slides were automatically scanned using an Olympus FV 3000 confocal microscope (Olympus, Tokyo, Japan), and the integrated optical density of fluorescent-labeled bacteria in hemocytes was quantified using ImageJ software (National Institutes of Health, Bethesda, MD, USA). The phagocytic index was calculated according to the equation provided in previous methods: Phagocytic index = mean fluorescence intensity of hemocytes in fluorescence-positive gate × (number of hemocytes in fluorescence-positive gate/total number of hemocytes) (Melcarne et al., 2019). At least five views were observed per sample, and the assay was performed three times.

2.10. Survival assay

At three days post-RNAi, the wasps were infected with bacteria as described above. Each group contained 20 wasps and was subsequently reared in an artificial climate chamber at 26 ± 1 °C. Since *M. mediator* has a short life span at room temperature, survival was recorded every 24 h for 5 days post-infection.

2.11. Statistical analysis

The data in this study were plotted using GraphPad Prism 5.0 (GraphPad Software, San Diego, CA, USA). One-way analysis of variance was used to analyze the significance of the expression levels of AMP genes (Fig. 2A) and *Mm*SR-B1 (Figs. 2B and 5A). The Student's *t*-test was used to determine differences between groups as shown in Fig. 5B–G as well as Fig. 6B and D. Data from the survival assay were analyzed using the log-rank (Mantel-Cox) test.

3. Results

3.1. MmS-B1 is a CD36/SR-B1 homolog

Protein family analysis using InterPro showed that the *Mm*SR-B1 homolog belongs to the SR-B1 family. Therefore, we compared the sequences of SR-B1 from octopus, sea cucumber, prawn, and zebrafish, in which SR-B1 was functionally studied (Fig. 1A). *Mm*SR-B1 shares approximately 30% identity with SR-B1s. *Mm*SR-B1 contains a CD36 domain and transmembrane segments at the N- and C- ends (Fig. 1B). We performed phylogenetic analysis of selected CD36/SR-B1 proteins from different insect species (the protein sequence alignment is provided in Supplemental File 1). They formed three subgroups: sensory neuron membrane proteins, croquemort, and SR-B1. The latter two also formed another group (Fig. 1C), suggesting that these two subgroups may originate from a common ancestor and possess the same functions.

3.2. Bacterial infection induces the expression levels of AMPs and MmSR-B1

Next, we performed RT-qPCR to analyze the antibacterial peptide and *Mm*SR-B1 mRNA levels in *M. mediator* that were challenged by the gram-negative bacterium *E. cloacae* and gram-positive bacterium *M. luteus*. The expression levels of *defensin 2*, *lysozyme 2*, *hymenoptaecin 1*, and *hymenoptaecin 2* significantly increased upon being challenged by *E. cloacae*. The expression levels of *defensin 2*, *lysozyme 1*, *hymenoptaecin*

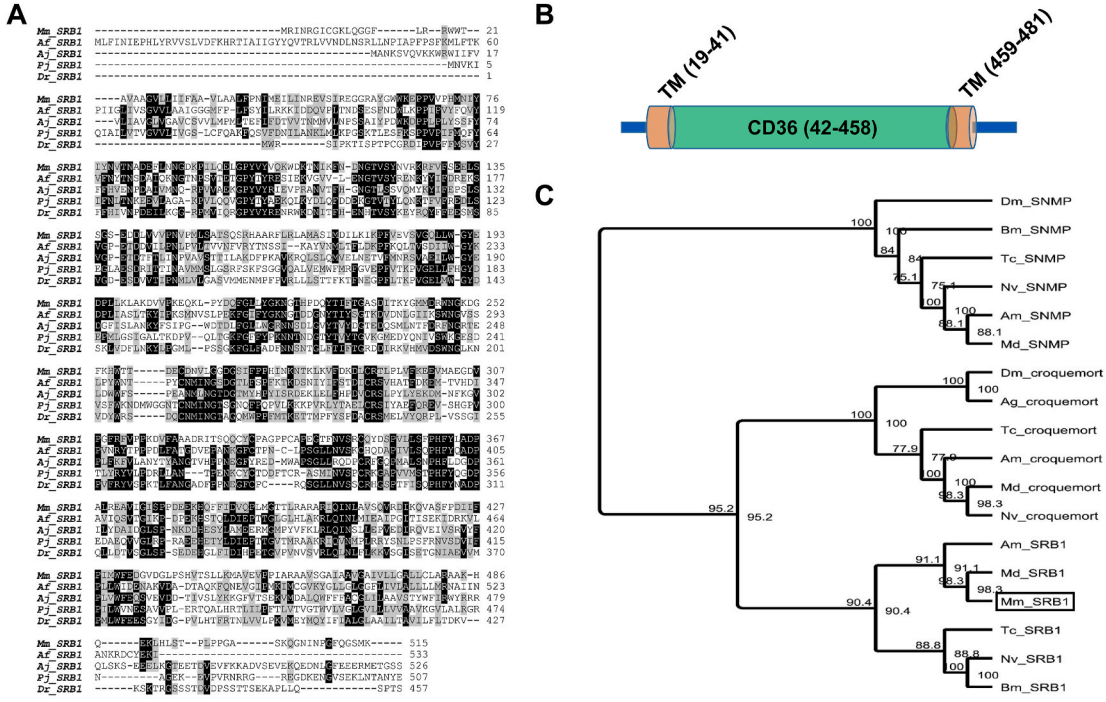

Fig. 1. Sequence comparison and phylogenetic analysis of CD36/SRB1 proteins. (A) Comparison of *Mm*_SRB1 sequence with SRB1 from octopus (Amphioctopus fangsiao, Af_SRB1, AWV50459.1), sea cucumber (Apostichopus japonicas, Aj_SRB1, AYO99755.1), Kuruma prawn (Penaeus japonicas, Pj_SRB1, AKO62849.1), and zebrafish (Danio rerio, Dr_SRB1, AAH44516.1). (B) Domain architecture of MmSRB1. TM, transmembrane region. The numbers in the parentheses indicate the amino acid residue positions in the protein sequence. (C) The phylogenetic tree of the CD36/SRB1 proteins in insects. The accession numbers of selected sequences are as follows: Md_SRB1, *Microplitis demolitor*, XP_014298816.1; Bm_SRB1, *Bombyx mori*, XP_012549834.1; Am_SRB1, *Apis mellifera*, XP_026301705.1; Tc_SRB1, *Tribolium castaneum*, NP_001164151.1; Nv_SRB1, *Nasonia vitripennis*, XP_032453704.1; Dm_croquemort, *Drosophila melanogaster*, NP_787957.1; Tc_croquemort, XP_975247.2; Ag_croquemort, *Anopheles gambiae*, AGAP010133-PA; *Am*_croquemort, XP_016767260.1; Md_croquemort, XP_008558638.1; Nv_croquemort, XP_031780045.1; Dm_SNMP, NP_650953.1; Bm_SNMP, NP_001037186.1; Tc_SNMP, EFA02899.2; Nv_SNMP, XP_001606602.1; Am_SNMP, XP_006562933.1; Md_SNMP, XP_008543235.2. These protein sequences were aligned using Clustal X2 program and the result is attached as the supplementary file.

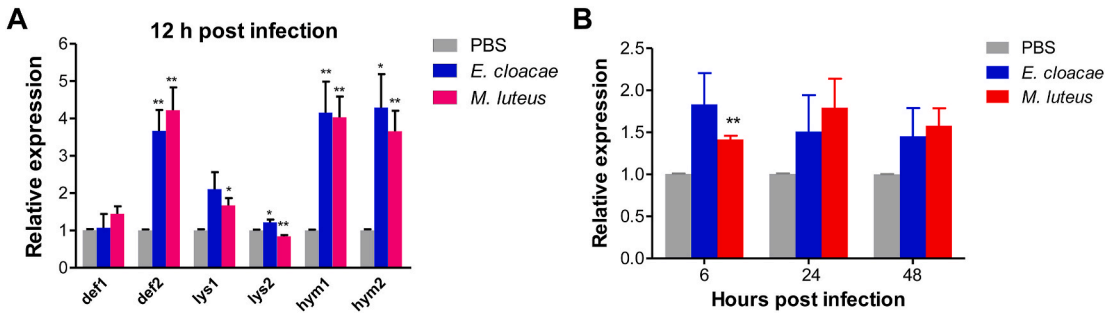

Fig. 2. Expression levels of antibacterial peptide genes (A) and *MmSR-B1* (B) in the infected *M. mediator*. At 12 h post infection, mRNA abundance of antibacterial peptide genes were determined in infected wasps. Def1: *defensin1*, def2: *defensin2*, lys1: *lysozyme1*, lys2: *lysozyme2*, hym1: *hymenoptaecin1*, hym2: *hymenoptaecin2*. To determine the temporal expression levels of *MmSR-B1*, wasps were collected at 6, 24, 48 h post *E. cloacae* and *M. luteus* infection, and control groups were treated with PBS. *Mmβ-actin* was used as an internal reference gene. The data were analyzed by one-way analysis of variance (ANOVA) (*$P < 0.05$, **$P < 0.01$).

1, and *hymenoptaecin 2* increased after *M. luteus* challenge. Interestingly, *M. luteus* infection decreased the expression level of *lysozyme 2* (Fig. 2A). *Mm*SR-B1 was upregulated at 6, 12, and 24 h post-infection (Fig. 2B), implying that *Mm*SR-B1 may be involved in *M. mediator* immune responses.

3.3. *MmSR-B1 binds to microbial ligands and causes agglutination of bacterial cells*

To further investigate its physiological function, the extracellular region of *Mm*SR-B1 was expressed in *E. coli* BL21 (DE3) cells. The molecular weight of recombinant *Mm*SR-B1 (r*Mm*SR-B1) was predicted to be approximately 47 kDa. After induction with IPTG, a large amount of protein was detected at 47 kDa in the inclusion body (Fig. 3A). After being verified by western blotting using anti-His monoclonal antibody (Fig. 3B), the r*Mm*SR-B1 protein was purified and renatured for functional assays.

An *in vitro* assay was carried out to determine the binding ability of r*Mm*SR-B1 to microbial ligands. The results showed that r*Mm*SR-B1 was strongly bound to the *Ec*-PG, *Bs*-PG, curdlan, *M. luteus*, and *P. aeruginosa* cells and weakly bound to the PG from *S. aureus* (Fig. 4A). In addition, r*Mm*SR-B1 was mixed with bacteria cells to test whether r*Mm*SR-B1 can cause agglutination of bacteria. Compared to BSA, r*Mm*SR-B1 caused agglutination of GFP-expressing *E. coli* and *P. aeruginosa* (Fig. 4B). These results suggest that *Mm*SR-B1 is involved in the binding and recognition of bacteria, thereby causing agglutination.

3.4. *MmSR-B1 mediates the expression levels of AMPs in the parasitoid*

To investigate the function of *Mm*SR-B1 in the wasp, we knocked down the *Mm*SR-B1 transcriptional level by RNAi. The efficiency of RNAi was confirmed by RT-qPCR at 2, 3, 4, and 5 days after dsRNA

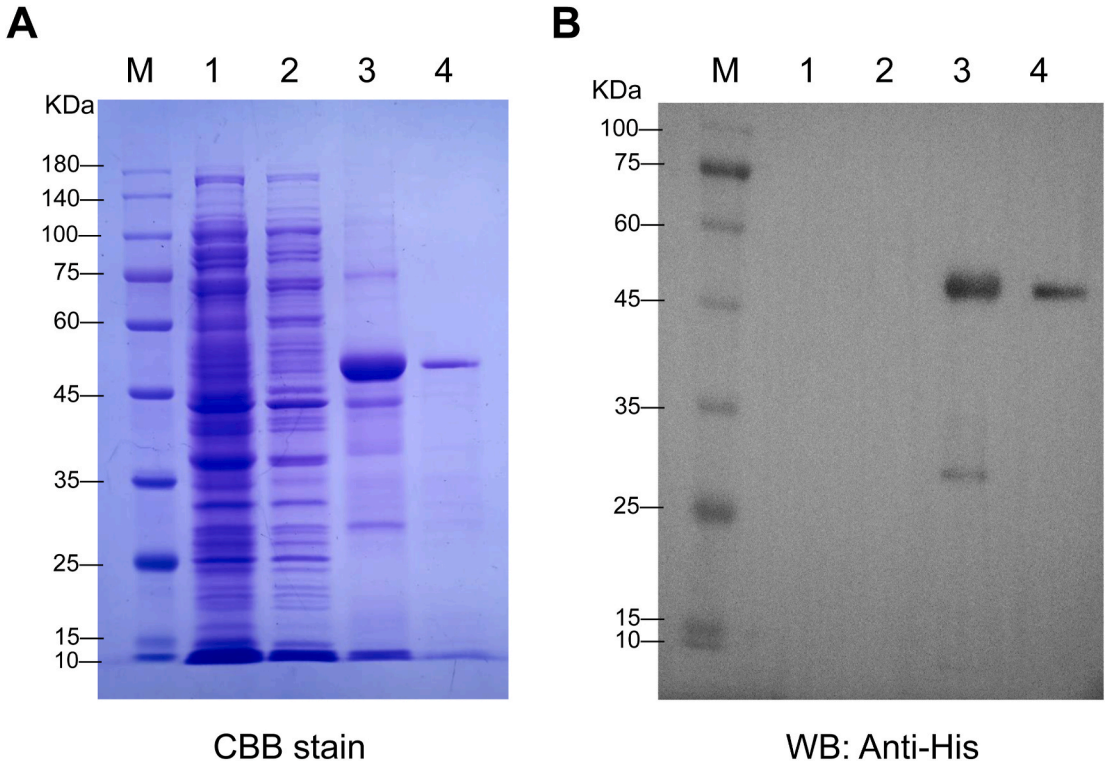

Fig. 3. Expression and purification of recombinant *Mm*SR-B1. In *E. coli* cells, *Mm*SR-B1 was expressed after 0.5 mM IPTG induction. The expression of *Mm*SR-B1 was analyzed by 10% SDS-PAGE (A) and verified by Western blot (B). Lane M, protein molecular weight markers; lane 1, proteins in non-induced *E. coli* harboring pET-28a-*Mm*SR-B1; lane 2, proteins in supernatant of induced *E. coli* pET-28a-*Mm*SR-B1; lane 3, proteins in inclusion body of induced *E. coli* pET-28a-*Mm*SR-B1; lane 4, purified and renatured r*Mm*SR-B1.

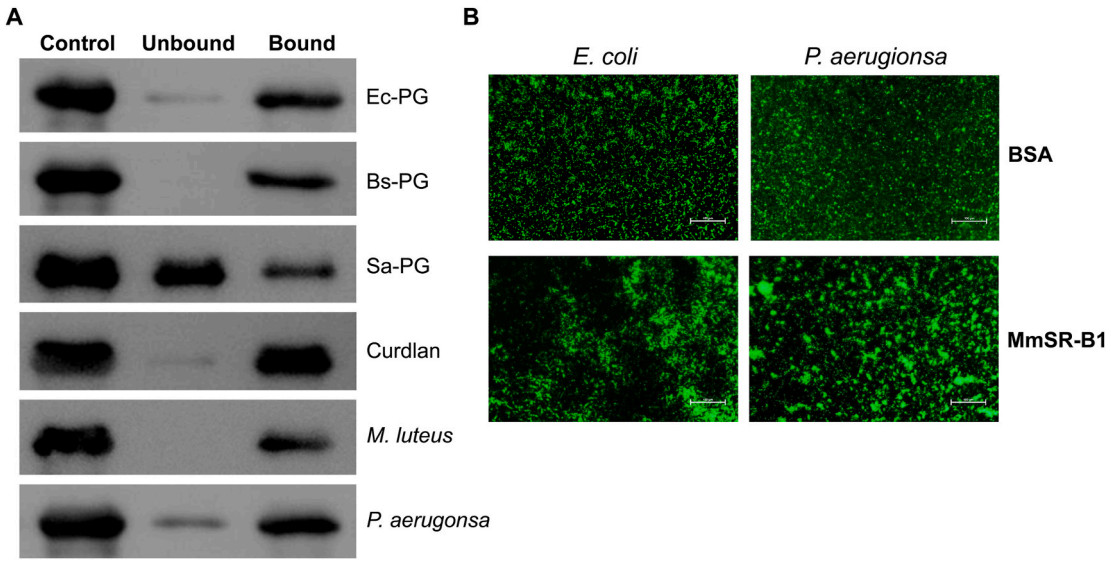

Fig. 4. *Mm*SR-B1 binds to microbial ligands and causes agglutination of bacteria. (A) Renatured r*Mm*SR-B1 was mixed with different microbial ligands, and then washed three times. The samples were separated by 10% SDS-PAGE, and analyzed by Western blotting using anti-His-tag monoclonal antibody. *Ec*-PG: *E. coli* PG, *Bs*-PG: *B. subtilis* PG, *Sa*-PG: *S. aureus* PG. (B) The GFP-expressing *E. coli* and *P. aeruginosa* were used to detect the agglutination ability of r*Mm*SR-B1, and BSA was used in the control group.

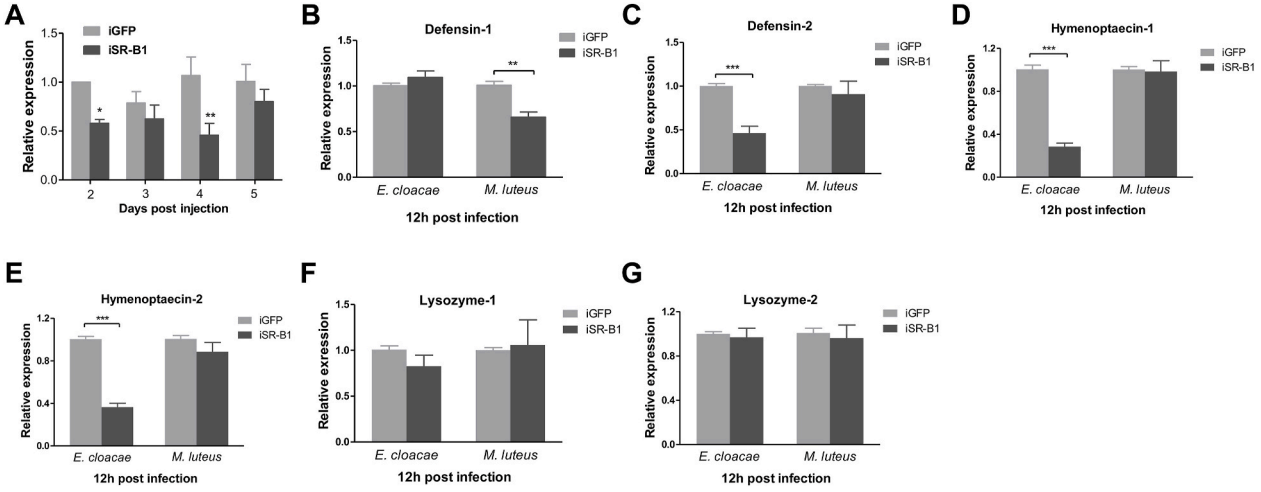

Fig. 5. *Mm*SR-B1 has positive impact on the expression of antibacterial peptide genes in *M. mediator*. Quantitative real-time PCR was performed to detect RNA interference efficiency at 2–5 d post dsRNA injection. Wasps injected with dsGFP were used as the control (A). At 3 d post RNA interference, wasps were infected with *E. cloacae* and *M. luteus*. The samples were collected at 12 h post infection, and the expression levels of *defensin* (B, C), *hymenoptaecin* (D, E) and *lysozyme* (F, G) were determined by qRT-PCR. The control group was injected with ds*GFP* and infected with the tested bacteria. Three biological replicates were performed. One-way analysis of variance (ANOVA) was used to analyze the statistical significance of the data in Fig. 5A (*$P < 0.05$, **$P < 0.01$). Pairwise comparisons were analyzed by Student's *t*-test in Fig. 5 B-G (**$P < 0.01$, ***$P < 0.001$).

injection. On the fourth day, the *Mm*SR-B1 expression level decreased by approximately 55% compared to that in the dsGFP-injected group (Fig. 5A). To examine whether *Mm*SR-B1 affects the expression levels of AMPs in *M. mediator*, we determined the changes in AMP mRNA levels after knockdown of *Mm*SR-B1 (Fig. 2A). As shown in Fig. 5B, the expression of *defensin 1* was reduced when the *Mm*SR-B1 knockdown wasps were challenged by *M. luteus* but not when infected by *E. cloacae*. However, the expression levels of *defensin 2* (Fig. 5C), *hymenoptaecin 1* (Fig. 5D) and *hymenoptaecin 2* (Fig. 5E) were reduced in response to *E. cloacae* infection in the *Mm*SR-B1 knockdown wasps. Knockdown of *Mm*SR-B1 had no effect on the expression of *lysozymes* (Fig. 5F and G). These results suggest that *Mm*SR-B1 mediates the expression levels of AMPs *defensin* and *hymenoptaecin* in the parasitoid.

3.5. *MmSR-B1 mediates phagocytosis of bacteria in the parasitoid*

To examine whether *Mm*SR-B1 mediates phagocytosis in the wasp, hemocytes from *Mm*SR-B1 knockdown wasps were incubated *in vitro* with fluorescent-labeled *E. coli* (Fig. 6A) and *S. aureus* (Fig. 6C). The results showed that knockdown of *Mm*SR-B1 significantly reduced the phagocytic ability of hemocytes from the wasps. Compared to the control groups, approximately 75% (for *E. coli*, Fig. 6B) and 85% (for *S. aureus*, Fig. 6D) reductions in the phagocytic index were found in the *Mm*SR-B1 knockdown wasps. Therefore, *Mm*SR-B1 mediates hemocyte phagocytosis.

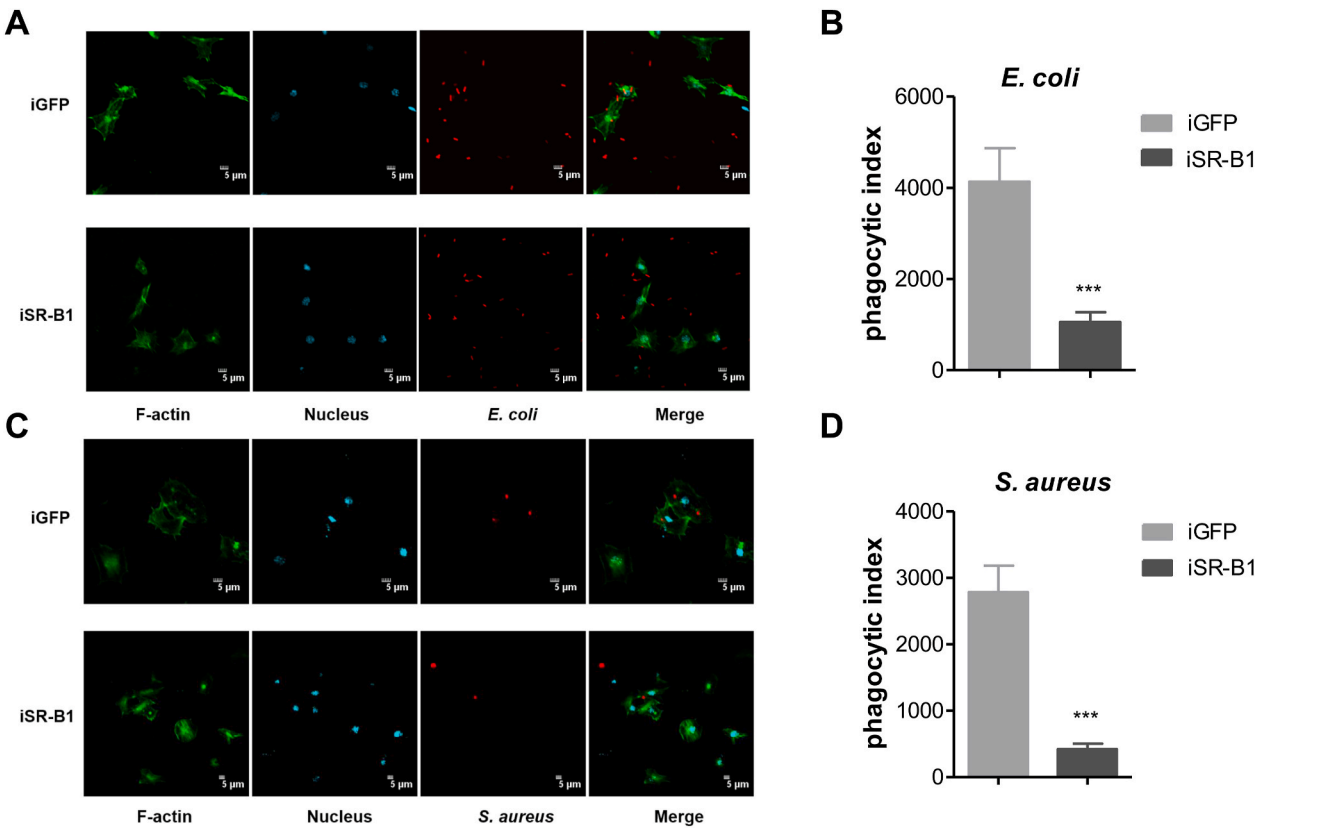

Fig. 6. *Mm*SR-B1 is required for phagocytosis of bacteria. Hemolymph was collected from dsRNA-injected wasps at 4 d, and incubated with Alexa 594-labeled *E. coli* (A) and *S. aureus* (red) (B). The F-actin was stained by SF488 phalloidin (green), and the cell nucleus was stained by hoechst 33342 (blue). Micrographs were captured on confocal microscope. Scale bar shown below the graph is 5 μm. The IOD value was determined by the Image J software and phagocytic index was calculated (C, D). Phagocytosis assay was repeated three times and at least 5 views were observed each time. Pairwise comparisons were analyzed by Student's *t*-test (***$P < 0.001$).

3.6. Knockdown of MmSR-B1 decreases wasp resistance to bacterial infection

Since we already found that *Mm*SR-B1 mediates AMP expression levels and hemocyte phagocytosis, two of the primary mechanisms for eliminating and removing invading pathogens, we next monitored the survival of the wasps after infection with *E. cloacae* (Fig. 7A) and *M. luteus* (Fig. 7B) for 5 days. There was no remarkable difference between the control groups and the *Mm*SR-B1 knockdown groups in the uninfected condition. After infection with bacteria, the survival of the *Mm*SR-B1 knockdown wasps was significantly reduced. Thus, our results suggest that *Mm*SR-B1 knockdown wasps are more susceptible to *E. cloacae* and *M. luteus* challenges.

4. Discussion

SR-Bs are known to mediate immune pathways and responses as a function of PRRs in vertebrates (Plüddemann et al., 2011; Silverstein and Febbraio, 2010; Prabhudas et al., 2014). Recently, several SR-Bs have been identified and investigated in shrimp (Bi et al., 2015), crabs (Yang et al., 2016; Wu et al., 2017; Kong et al., 2018), sea cucumbers (Che et al., 2019), and octopus (Wei et al., 2018). SR-B has not been reported in insects; however, it has been shown that SR-B-related croquemorts are required for phagocytosis in *Drosophila* (Franc et al., 1999; Stuart et al., 2005). Mosquito *Anopheles gambiae* croquemort SCRBQ2 is involved in *Plasmodium*–mosquito interactions (González-Lázaro et al., 2009). Because SR-Bs and croquemorts form a group in phylogenetic analysis (Fig. 1C), we speculated that SR-Bs may possess functions similar to those of croquemorts.

In this study, we demonstrated for the first time that SR-B1 from the parasitic wasp *M. mediator* binds to PAMPs, causing agglutination of bacteria, involvement in hemocyte phagocytosis, and regulation of AMP expression levels. The recombinant CD36 domain of *Mm*SR-B1 demonstrated binding to PGs from *E. coli* and *B. subtilis* as well as curdlan from *A. faecalis* (Fig. 4A). SR-B from swimming crabs showed high affinity for PG and lipoteichoic acid (LTA) but low affinity for lipopolysaccharide (LPS) (Yang et al., 2016). SR-B from sea cucumbers showed high affinity for LPS (Che et al., 2019), and SR-B1 from shrimp could bind to LPS and LTA but not to PG (Bi et al., 2015). Therefore, the binding specificity and capacity of SR-Bs may vary among different species. Our RNAi experiment indicated that *Mm*SR-B1 promotes the phagocytosis of bacterial cells in wasps (Fig. 6). The C-terminal cytoplasmic region of the croquemort is required for phagocytosis by *S. aureus* in *Drosophila* (Stuart et al., 2005). In shrimp, deletion of the C-terminal region of SR-B1 impaired bacterial clearance (Bi et al., 2015). Thus, it is likely that the C-terminal region of *Mm*SR-B1 is critical for its role in phagocytosis.

Several studies have suggested that SR-B1 is involved in the regulation of the AMP pathway, likely through interaction with TLRs (Bi et al., 2015; Kong et al., 2018; Wei et al., 2018; Tang et al., 2020). Similarly, we found that knockdown of *Mm*SR-B1 resulted in the downregulation of *defensin* and *hymenoptaecin* expression levels in wasps (Fig. 5), confirming its involvement in the regulation of AMP pathways. Interestingly, this regulation showed some specificity. The expression levels of *defensin 2*, *hymenoptaecin 1*, and *hymenoptaecin 2* were induced by *E. cloacae* and *M. luteus* infections (Fig. 2A), but knockdown of *Mm*SR-B1 affected their expression only when the wasps were infected with *E. cloacae* (Fig. 5C–E). These results imply that these AMPs are generated through distinct pathways and *that Mm*SR-B1 regulates

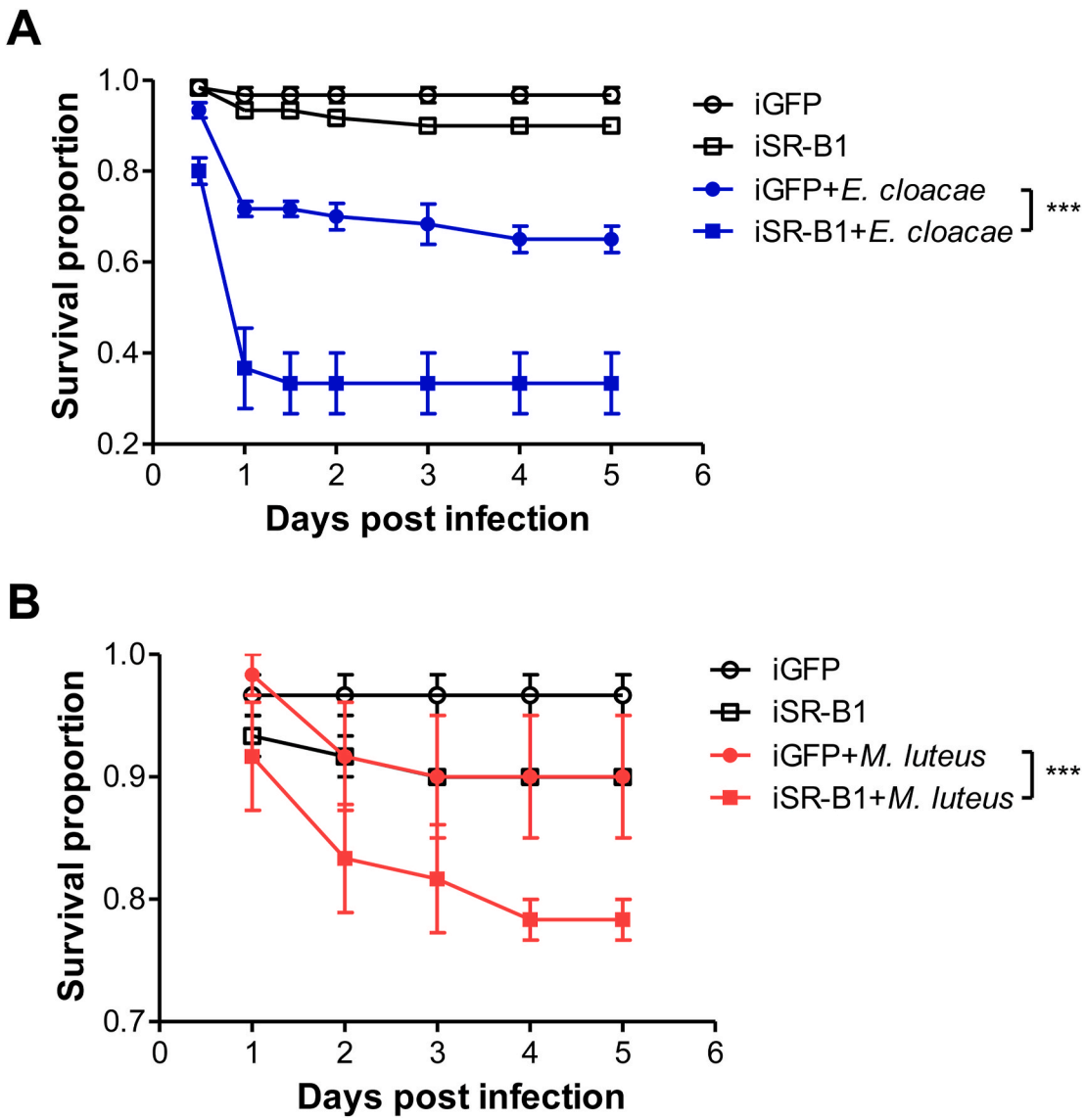

Fig. 7. Effect of MmSR-B1 on wasps' survival after bacterial infection. At 3 d post. dsRNA injection, wasps were infected with *E. cloacae* (A) and M. luteus (B), and survival rate was recorded every day for 5 days. Three biological replicates were performed. Difference between groups were analyzed with a long-rank (Mantel-Cox) test (***P < 0.001).

specific pathways.

In summary, we showed that SR-B1 is involved in hemocyte phagocytosis and regulation of AMP production. It plays an important role in the defense against bacterial infection in the parasitic wasp *M. mediator*.

Author contributions

Z.L. and L.Z.Z. designed research; L.Z.Z., R.J.W., Y.Y.Y. and S.Z. preformed research; L.Z.Z. and Z.L. analyzed the data; L.Z.Z., Z.L. and Z. Z. wrote the manuscript.

Funding

This work was supported by National Natural Science Foundation of China grants 31772530 and 31970467 to ZL. The funder had no role in study design, data collection and analysis, decision to publish, or preparation of the manuscript.

Appendix A. Supplementary data

Supplementary data to this article can be found online at https://doi.org/10.1016/j.dci.2021.104039.

References

Bi, W.J., Li, D.X., Xu, Y.H., Xu, S., Li, J., Zhao, X.F., Wang, J.X., 2015. Scavenger receptor B protects shrimp from bacteria by enhancing phagocytosis and regulating expression of antimicrobial peptides. Dev. Comp. Immunol. 51, 10–21.

Buchon, N., Silverman, N., Cherry, S., 2014. Immunity in *Drosophila melanogaster*-from microbial recognition to whole-organism physiology. Nat. Rev. Immunol. 14, 796–810.

Canton, J., Neculai, D., Grinstein, S., 2013. Scavenger receptors in homeostasis and immunity. Nat. Rev. Immunol. 13, 621–634.

Che, Z., Shao, Y., Zhang, W., Zhao, X., Guo, M., Li, C., 2019. Cloning and functional analysis of scavenger receptor B gene from the sea cucumber *Apostichopus japonicus*. Dev. Comp. Immunol. 99, 103404.

Chen, K., Zhou, L., Chen, F., Peng, Y., Lu, Z., 2016. Peptidoglycan recognition protein-S5 functions as a negative regulator of the antimicrobial peptide pathway in the silkworm, *Bombyx mori*. Dev. Comp. Immunol. 61, 126–135.

Franc, N.C., Heitzler, P., Ezekowitz, R.A., White, K., 1999. Requirement for croquemort in phagocytosis of apoptotic cells in *Drosophila*. Science 284, 1991–1994.

Goldstein, J.L., Ho, Y.K., Basu, S.K., Brown, M.S., 1979. Binding site on macrophages that mediates uptake and degradation of acetylated low density lipoprotein, producing massive cholesterol deposition. Proc. Natl. Acad. Sci. Unit. States Am. 76, 333–337.

González-Lázaro, M., Dinglasan, R.R., Hernández-Hernández, F., Rodríguez, M.H., Laclaustra, M., Jacobs-Lorena, M., Flores-Romo, L., 2009. *Anopheles gambiae* Croquemort SCRBQ2, expression profile in the mosquito and its potential interaction with the malaria parasite Plasmodium berghei. Insect Biochem. Mol. Biol. 39, 395–402.

Gough, P.J., Gordon, S., 2000. The role of scavenger receptors in the innate immune system. Microb. Infect. 2, 305–311.

Guillou, A., Troha, K., Wang, H., Franc, N.C., Buchon, N., 2016. The *Drosophila* CD36 homologue croquemort is required to maintain immune and gut homeostasis during development and aging. PLoS Pathog. 12, e1005961.

Hanson, M.A., Lemaitre, B., 2020. New insights on *Drosophila* antimicrobial peptide function in host defense and beyond. Curr. Opin. Immunol. 62, 22–30.

Hillyer, J.F., 2016. Insect immunology and hematopoiesis. Dev. Comp. Immunol. 58, 102–118.

Hillyer, J.F., Strand, M.R., 2014. Mosquito hemocyte-mediated immune responses. Curr. Opin. Insect 3, 14–21.

Huang, Y., Ren, Q., 2020. Research progress in innate immunity of freshwater crustaceans. Dev. Comp. Immunol. 104, 103569.

Kocks, C., Cho, J.H., Nehme, N., Pearson, A.M., Meister, M., Strom, C., Conto, S.L., Hetru, C., Stuart, L.M., Stehle, T., Hoffmann, J.A., Reichhart, J.M., Ferrandon, D., Rämet, M., Ezekowitz, R.A.B., 2005. Eater, a transmembrane protein mediating phagocytosis of bacterial pathogens in *Drosophila*. Cell 123, 335–346.

Kong, T., Gong, Y., Liu, Y., Wen, X., Tran, N.T., Aweya, J.J., Zhang, Y., Ma, H., Zheng, H., Li, S., 2018. Scavenger receptor B promotes bacteria clearance by enhancing phagocytosis and attenuates white spot syndrome virus proliferation in *Scylla paramamosian*. Fish Shellfish Immunol. 78, 79–90.

Lin, Z., Cheng, Y., Wang, R.-J., Du, J., Volovych, O., Li, J.-C., Hu, Y., Lu, Z.-Y., Lu, Z., Zou, Z., 2018. A metalloprotease homolog venom protein from a parasitoid wasp suppresses the Toll pathway in host hemocytes. Front. Immunol. 9, 2301. https://doi.org/10.3389/fimmu.2018.02301.

Lin, Z., Wang, R.J., Cheng, Y., Du, J., Volovych, O., Han, L.B., Li, J.C., Hu, Y., Lu, Z.Y., Lu, Z., Zou, Z., 2019. Insights into the venom protein components of *Microplitis mediator*, an endoparasitoid wasp. Insect Biochem. Mol. Biol. 105, 33–42. https://doi.org/10.1016/j.ibmb.2018.12.013.

Lu, Y., Su, F., Li, Q., Zhang, J., Li, Y., Tang, T., Hu, Q., Yu, X.Q., 2020. Pattern recognition receptors in Drosophila immune responses. Dev. Comp. Immunol. 102, 103468.

Ma, L., Liu, L., Zhao, Y., Yang, L., Chen, C., Li, Z., Lu, Z., 2020. JNK pathway plays a key role in the immune system of the pea aphid and is regulated by microRNA-184. PLoS Pathog. 16, e1008627.

Melcarne, C., Ramond, E., Dudzic, J., Bretscher, A.J., Andó, I., Lemaitre, B., 2019. Two Nimrod receptors, NimC1 and Eater, synergistically contribute to bacterial phagocytosis in *Drosophila melanogaster*. FEBS J. 286, 2670–2691.

Meng, Q., Zhang, J.H., Zhang, H., Zhou, G.L., Ni, R.Y., Zhao, Y.N., Qin, Q.L., Zou, Z., 2018. Comparative analysis of C-type lectin domain proteins in the ghost moth, *Thitarodes xiaojinensis* (Lepidoptera: Hepialidae). Insect Sci. 26 (3), 453–465. https://doi.org/10.1111/1744-7917.12564.

Mukhopadhyay, S., Gordon, S., 2004. The role of scavenger receptors in pathogen recognition and innate immunity. Immunobiology 209, 39–49.

Neculai, D., Schwake, M., Ravichandran, M., Zunke, F., Collins, R.F., Peters, J., Neculai, M., Plumb, J., Loppnau, P., Pizarro, J.C., Seitova, A., Trimble, W.S., Saftig, P., Grinstein, S., Dhe-Paganon, S., 2013. Structure of LIMP-2 provides functional insights with implications for SR-BI and CD36. Nature 504, 172–176.

Peiser, L., Mukhopadhyay, S., Gordon, S., 2002. Scavenger receptors in innate immunity. Curr. Opin. Immunol. 14, 123–128.

Plüddemann, A., Mukhopadhyay, S., Gordon, S., 2011. Innate immunity to intracellular pathogens: macrophage receptors and responses to microbial entry. Immunol. Rev. 240, 11–24.

Prabhudas, M., Bowdish, D., Drickamer, K., Febbraio, M., Herz, J., Kobzik, L., Krieger, M., Loike, J., Means, T.K., Moestrup, S.K., Post, S., Sawamura, T., Silverstein, S., W, X.Y., Khoury, J.E., 2014. Standardizing scavenger receptor nomenclature. J. Immunol. 192, 1997–2006.

Rosales, C., 2011. Phagocytosis, a cellular immune response in insects. ISJ-Invert. Surviv. J. 8, 109–131.

Schmittgen, T.D., Livak, K.J., 2008. Analyzing real-time PCR data by the comparative C (T) method. Nat. Protoc. 3, 1101–1108.

Shen, W.J., Hu, J., Hu, Z., Kraemer, F.B., Azhar, S., 2014. Scavenger receptor class B type I (SR-BI): a versatile receptor with multiple functions and actions. Metabolism 63, 875–886.

Silverstein, R.L., Febbraio, M., 2010. CD36, a scavenger receptor involved in immunity, metabolism, angiogenesis, and behavior. Sci. Signal. 2, re3.

Stewart, C.R., Stuart, L.M., Wilkinson, K., Gils, J.M., Deng, J., Halle, A., Rayner, K.J., Boyer, L., Zhong, R., Frazier, W.A., Lacy-Hulbert, A., Khoury, J.E., Golenbock, D.T., Moore, K.J., 2010. CD36 ligands promote sterile inflammation through assembly of a Toll-like receptor 4 and 6 heterodimer. Nat. Immunol. 11, 155–161.

Strand, M.R., 2008. The insect cellular immune response. Insect Sci. 15, 1–14.

Stuart, L.M., Deng, J., Silver, J.M., Takahashi, K., Tseng, A.A., Hennessy, E.J., Ezekowitz, R.A., Moore, K.J., 2005. Response to *Staphylococcus aureus* requires CD36-mediated phagocytosis triggered by the COOH-terminal cytoplasmic domain. J. Cell Biol. 170, 477–485.

Tang, M., Li, X., Yang, L., Wang, Q., Li, W., 2020. A class B scavenger receptor mediates antimicrobial peptide secretion and phagocytosis in Chinese mitten crab (*Eriocheir sinensis*). Dev. Comp. Immunol. 103, 103496.

Wang, R.J., Lin, Z., Jiang, H., Li, J., Saha, T.T., Lu, Z., Lu, Z., Zou, Z., 2017. Comparative analysis of peptidoglycan recognition proteins in endoparasitoid wasp *Microplitis mediator*. Insect Sci. 24, 2–16.

Wei, X., Zhao, T., Ai, K., Li, H., Jiang, X., Li, C., Wang, Q., Yang, J., Zhang, R., Yang, J., 2018. Role of scavenger receptor from *Octopus ocellatus* as a co-receptor of Toll-like receptor in initiation of TLR-NF-κB signaling during anti-bacterial response. Dev. Comp. Immunol. 84, 14–27.

Wu, Y.M., Yang, L., Li, X.J., Li, L., Wang, Q., Li, W.W., 2017. A class B scavenger receptor from *Eriocheir sinensis* (EsSR-B1) restricts bacteria proliferation by promoting phagocytosis. Fish Shellfish Immunol. 70, 426–436.

Yang, N., Zhang, D.F., Tao, Z., Li, M., Zhou, S.M., Wang, G.L., 2016. Identification of a novel class B scavenger receptor homologue in *Portunus trituberculatus*: molecular cloning and microbial ligand binding. Fish Shellfish Immunol. 58, 73–81.

Yi, H.Y., Chowdhury, M., Huang, Y.D., Yu, X.Q., 2014. Insect antimicrobial peptides and their applications. Appl. Microbiol. Biotechnol. 98, 5807–5822.

Zheng, Z., Ai, J., Li, X.A., 2014. Scavenger receptor class B type I and immune dysfunctions. Curr. Opin. Endocrinol. Diabetes Obes. 21, 121–128.